



# Unique identification of gold and banknotes through the use of antipode elements: Material selection, laboratory verification steps, and industrial software–hardware implementation ☆☆☆

Athanasios Zisopoulos\*, Georgia Broni, Nikos Kartalis, Konstandinos Panitsidis

Department of Management and Technology Studies, University of Western Macedonia, Faculty of Economic Sciences, Kila Campus, Kozani 50100, Greece

## REVIEW HIGHLIGHTS

- In the first part of this research, we analyze the distinguishing Mendelev elements and commercially available materials for "volume magnetic susceptibility" with a simple bibliographical analysis of antipodal elements and electric resistivity inside a piece of paper.
- In the last part, we present the same basic Antipodal method for gold and paper. The validation for gold has stages for casting and assembly for a radiographic device. The method for handmade paper sheets has steps that include infusion with Antipodal ingredients, lab X-ray machine, raw, direct sensor, and digital electronic tools.

## ARTICLE INFO

### Method name:

Antipodal: Antipode identification using pre-embodied ingredients inside gold and banknotes to provide distinguishability and traceability

### Keywords:

Econophysics  
Gold identification  
Traceable ingredients  
Antipode materials

## ABSTRACT

The falsification problems associated with golden coins, banknotes, and legal documents could be solved through "antipode elements," microfiber materials selected to have the exact opposite (antipode) properties when incorporated into gold, paper, or any other tangible manufactured object. Any discrepancies in gold or banknotes could be found using various non-destructive testing machinery. This research focus was given to help a student or junior lab technician replicate all steps and conclude that a fully functional product is ready for the alpha test. It requires minimal interdisciplinary knowledge in statistics, programming, and metrology, along with chemical, material, and digital electronics engineering. The research methodology can be categorized into four tracks: material selection and method validation. The two validation steps were kept short and low level, that is, minimal and only to guide reproducibility, due to limitations in presentation, procedural specification, pricing, consumable options, and software modules. A last-minute development occurred by describing the procedures in the current submission, not initially granted in the invention patents. This technique is an innovative design to capture raw sensor data straight from the photodiode pad. These Big-Data are manipulated using the presented and future data analytics methodologies.

☆ Related research article

☆☆ For a published article: Zisopoulos, A. (2021). MIDAS, Repository with "Under the Pillow Gold" Using Antipodal Unique Identification of Golden Coins for Regional Development and Monetary Applications. *Review of International Geographical Education*, 12(01), 2022. <https://rigeo.org/menu-script/index.php/rigeo/article/view/472>, [https://papers.ssrn.com/sol3/papers.cfm?abstract\\_id=4092050](https://papers.ssrn.com/sol3/papers.cfm?abstract_id=4092050).

\* Corresponding author.

E-mail address: [a.zisopoulos@uowm.gr](mailto:a.zisopoulos@uowm.gr) (A. Zisopoulos).

## Specifications table

Subject area	Computer Science
Specific subject area	Economics and Finance Materials Science
Method	Antipodal: Antipode identification using pre-embodied ingredients inside gold and banknotes to provide distinguishability and traceability
Original method and reference	GR1010167 GOLD BULLION ORIGATION AND VERIFICATION SYSTEM WITH UNIQUE IDENTIFICATION BY EMBEDDING TRACEABLE INGREDIENTS. (n.d.). Retrieved September 24, 2022, from <a href="https://patentscope.wipo.int/search/en/detail.jsf?docId=GR356981880&amp;_cid=P11-L8G199-08661-1">https://patentscope.wipo.int/search/en/detail.jsf?docId=GR356981880&amp;_cid=P11-L8G199-08661-1</a> Grant Number: 1010167, Grant Date: 31.01.2022 GR1010230 PAPER PULP METHODOLOGY FOR PRODUCTION OF UNIQUE PAPER SHEETS AND BANKNOTES EMBODIED WITH EXCLUSIVITY ANTIPODE TRACE ELEMENTS. (n.d.). Retrieved September 24, 2022, from <a href="https://patentscope.wipo.int/search/en/detail.jsf?docId=GR367948438&amp;_cid=P11-L8G199-08661-1">https://patentscope.wipo.int/search/en/detail.jsf?docId=GR367948438&amp;_cid=P11-L8G199-08661-1</a> Grant Number: 1010230, Grant Date: 06.05.2022
Resource availability	<a href="https://data.mendeley.com/datasets/mgr25gs4k6">https://data.mendeley.com/datasets/mgr25gs4k6</a> <a href="https://data.mendeley.com/datasets/2592m8ctp6">https://data.mendeley.com/datasets/2592m8ctp6</a> <a href="https://data.mendeley.com/datasets/j3762k2f46">https://data.mendeley.com/datasets/j3762k2f46</a> <a href="https://www.hamamatsu.com/content/dam/hamamatsu-photonics/sites/documents/99_SALES_LIBRARY/ssd/x-ray_kmpd9016e.pdf">https://www.hamamatsu.com/content/dam/hamamatsu-photonics/sites/documents/99_SALES_LIBRARY/ssd/x-ray_kmpd9016e.pdf</a>

## Method details

The Mathematical approach for anomaly detection has various usages. For example, the banking world uses this detection to reduce gold and banknote forgery. Usually, gold or banknote surface anomalies reveal falsification. However, this procedure is reversed, and tiny fiber anomalies are incorporated during casting inside gold. These tiny fibers or similar chemical traceable ingredients are visible through various techniques measuring physical, chemical, and radiographic properties.

These 41 properties are described in the third sheet of the primary dataset [1] for Mendelev periodic table elements. Most of these properties also concern earth and artificial materials. For the current application, only fourteen properties of the elements are eligible: Electrical Conductivity, Electronegativity, Heat of Fusion, Heat of Vaporization, Melting Point, Specific Heat, Color, Electrical Type, Magnetic Type, Mass Magnetic Susceptibility, Resistivity, Speed of Sound, Thermal Conductivity and Volume Magnetic Susceptibility. The initial methodology searches for the distinction points between any mixture of two elements. The procedure theoretically is:

- First, the element property is chosen, for example, resistivity.
- Then for the selected property, two materials are chosen, for example, Gold and Sulfur.
- Finally, we create a mixture of the two materials, for example, a golden coin.

This coin is uniquely identifiable in an appropriate scanner.

Golden coins, banknotes, and office documents all face forgery problems. Financial Intelligence units around the world endorse digital forensic methods. So-called “antipode elements” constitute one solution to the problem. After thorough analysis, several micro-materials selected to have the exact opposite (antipodal) properties were incorporated into gold and paper. The gold became uniquely identifiable through various non-destructive testing (NDT) machinery sheets involving radiography, visual, ultrasonic, currencies, acoustics, and magnetics. The method applies to the following areas:

1. Gold and security items.
2. Banknotes and necessary official paperwork.
3. Any tangible artificial item.
4. Preprocessed food.

All existing patents and scientific studies [7,9,10,11] published in scientific journals on MethodsX Scientific Journal have contributed to the overall understanding, subsystem design, and experimental research verification.

The current research gives specific guidelines and laboratory steps for a non-experienced user to accommodate all necessary research steps. The article’s purpose and writing altitude are technical, educational, and brainstorming for similar research and products.

## ALPHA

*ALPHA-I-step: analysis to distinguish Mendelev elements*

The dataset “Mendelev–antipode-properties” [1], which lists the 41 basic properties of the 118 universal Mendelev elements, was used for this method. The columns show the property, the element, the numeric value, and appropriate metric units. The 4838 rows indicate all possible property–element combinations. The dataset is useful for preliminary material studies to find pairs for traceability applications and engineering. A short list of properties was selected for a concise presentation, limited to the Mendelev periodic table.

The selection list of materials’ properties included melting point, electrical conductivity, electronegativity, the heat of fusion, bulk modulus, magnetic type, and mass magnetic susceptibility. Of course, the elements will have more properties and materials. Four discrete steps are described for methodology clarification, with up to eleven total implementation steps.

**Table 1**  
Elements' distance from gold to ascertain volume magnetic susceptibility.

Element	Value	Gold	Distance
Copper	−102.3	−3.44E−05	102
Germanium	−85.8	−3.44E−05	86
Hydrogen	−31.3	−3.44E−05	31
Chlorine	−31.1	−3.44E−05	31
Helium	−19.5	−3.44E−05	19
Argon	−18.7	−3.44E−05	19
Holmium	0.048285	−3.44E−05	0
All others			0

**Table 2**  
Melting points of elements melted after gold.

Element	Value	Gold	Distance
Carbon	3.55E+03	1064	−2486
Tungsten	3422	1064	−2358
...			
Gadolinium	1.31E+03	1064	−249
Beryllium	1.29E+03	1064	−223
Manganese	1.25E+03	1064	−182
Americium	1.18E+03	1064	−112
Uranium	1135	1064	−71
Promethium	1100	1064	−36
Copper	1.08E+03	1064	−20
Samarium	1072	1064	−8
Gold	1.06E+03	1064	0

**Table 3**  
Magnetic and melting distances above that of gold.

Element	Volume magnetic susceptibility	Melting point
Copper	102	−20.44
Germanium	86	125.88
Hydrogen	31	1323.32
Chlorine	31	1165.68
Argon	19	1253.48
Holmium	0	−409.82
Dysprosium	0	−347.82

#### ALPHA-II-step: bibliographical analysis of elements to ascertain volume magnetic susceptibility in gold

For Alpha [1], lines 4604–4721 of the dataset show the elements' volume magnetic susceptibilities. Table 1 summarizes every element's antipode distance from gold, that is, the difference between gold and each element.

In the dataset, lines 1536–1653 show the melting points of the Mendeleev elements in degrees Celsius.

Based on Tables 1 and 2, decision Table 3 shows that a thin line of engineering intervenes in realizing the impossible. Magnetic susceptibility as a distinguishability in gold bullion only applies in the case of one element.

The overall result of Alpha-II suggests that while magnetic susceptibility is an excellent academic experiment, there are other candidates for application to actual market products. However, the 20-degree difference in the melting point of the copper-gold pair imposes restrictions and incurs costs regarding casting and enrichment.

#### ALPHA-III-step: bibliographical analysis of antipodal elements to ascertain electric resistivity inside the paper

Regarding Alpha [1], in the dataset, lines 3542–3659 show the essential elements' resistivities. Electric resistivity is measured with non-destructive testing (NDT) sensors. A different and uncomplicated approach is used for antipodal ingredients added to the paper. Table 4 presents the elements' resistivity in m-Ohm ( $\Omega$ ). According to this classification, a handful of elements have the desired property, while all the others are worthless.

Only five elements are eligible for incorporation into the paper as antipode elements. Since additive ingredients will be incorporated into the paper, it is necessary to investigate the capacity for incorporation into melted paper pulp. Paper pulp processing requires high temperatures to mix the paper. However, NDT antipode ingredients can be placed in the pulp at the final stage, when the temperature is significantly lower, at 115°. Table 5 shows the pre-selected materials' melting points in Celsius.

**Table 4**  
Content of the first and last columns showing the elements' electric resistivity.

Classification	Element	Value (in m $\Omega$ )
1	Sulfur	1,000,000,000,000,000
2	Bromine	10,000,000,000
3	Iodine	10,000,000
4	Boron	10,000
5	Chlorine	100
6	Silicon	0.001
...	...	..
79	Gold	0.000000022
80	Copper	0.000000017
81	Silver	0.000000016

**Table 5**  
Melting points of pre-selected high-resistivity elements.

Element	Melting point (in degrees Celsius)
Sulfur	115.21
Bromine	−7.3
Iodine	113.7
Boron	2075

It was found that sulfur is suitable for use as an antipode ingredient in banknotes and necessary paper-based contracts because it has the highest absolute electric resistivity and can be easily incorporated at the last stage of banknote paper pulp processing.

### BETA-step: analysis of real-world material

Mendeleev table elements are not suitable for industrial applications. Purity does not exist in nature. The Material 1 selection list is more complex than an academic experiment with Mendeleev table generalizations. A universal tool for material selection is MATWEB [4]. After completion of the first scientific steps, engineering follows. Preparing a decent Big Data representation of available industrial materials and studying them is a lifetime task. In many ways, it is similar to that undertaken initially by the inspired Mendeleev pioneer.

The methodology's second step entails studying the material properties database and identifying a suitable pair with distinct antipodal properties. The Big Data material database contains 141,869 records commercially available in various classes: carbon, ceramic, fluid, metal, engineering material, polymers, and pure elements. The big difference compared to the previous academic step is that realization is necessary. The material pair is still to be found and is valuable for industrial applications. The material list may not include gold and banknotes but any omnifarious tangible article with traceable ingredients.

The preferred method to locate the desirable "antipode trail" in Data Science is always a well-structured SQL query. However, for copyright reasons, this is not possible. The second-best tool is a MATWEB query, which lacks the scientific value of SQL but is amenable to this preliminary trial implementation.

This step entailed a simple web query to locate the desired material pair with maximum distinguishability. The base query searched 30,440 materials for the following three properties: electrical resistivity, melt temperature, and heat of fusion (<https://www.matweb.com/search/PropertySearch.aspx>).

The exact query is shown in 1Fig. 1, with the following arguments:

- First, find the electric resistivity of 30,440 materials with minimum resistivity of 0.000001 OHM and max infinitive.
- Find the melting temperature of 27,542 materials above 100 °C.
- Find the heat of fusion in the range of 5–1000 J/g.

The query shown in Fig. 11 returned many materials, the first ten of which are shown in Fig. 2. Table 6 shows the properties of the first item, "Braskem polyethylene."

All results are given in a non-structured format as brainstorming information with detailed specifications and a first draft to proceed to material analysis. To replicate the steps are:

1. Initially, locate the materials through marketing analysis, focusing on aspects such as availability and pricing.
2. Laboratory tests any desired property and generates a "behavioral material archetype" using a computer.
3. Several such archetypes could be in a manipulatable form to select an antipodal pair of real-world materials.

**Electrical Resistivity (30440 matis)**

Min:  Max:  Unit:

Min: [1.00e-6 ohm-cm](#)  
Max: [1.60e+25 ohm-cm](#)

**Melt Temperature (27542 matis)**

Min:  Max:  Unit:

Min: [40.0 °C](#)  
Max: [816 °C](#)

**Heat of Fusion (1070 matis)**

Min:  Max:  Unit:

Min: [1.50 J/g](#)  
Max: [9740 J/g](#)

Fig. 1. The initial MATWEB query with three properties.

Material Name	Electrical Resistivity (ohm-cm)	Melt Temperature (°C)	Heat of Fusion (J/g)
<a href="#">Braskem UTEC® 6540 Ultra High Molecular Weight Polyethylene</a>	1.00e+14	133	68.3
<a href="#">Eastman 7352 PET</a>	1.00e+16	275 - 295	63.0
<a href="#">Eastman Ecdel PCCE 9966 Copolyester Ether Elastomer</a>	1.00e+14	307	27.0
<a href="#">Solvay Specialty Polymers Hyflon® MFA 1041 Perfluoroalkoxy (PFA)</a>	1.00e+17	250 - 400	18.0 - 26.0
<a href="#">Solvay Specialty Polymers Hyflon® MFA F1540 Perfluoropolymer</a>	1.00e+17	240 - 420	16.0 - 24.0
<a href="#">Solvay Specialty Polymers Hyflon® PFA F1520 Perfluoropolymer</a>	1.00e+17	240 - 400	16.0 - 24.0
<a href="#">Solvay Specialty Polymers Hyflon® F1520 Perfluoropolymer</a>	1.00e+17	240 - 400	16.0 - 24.0
<a href="#">Solvay Specialty Polymers Hyflon® F1540 Perfluoropolymer</a>	1.00e+17	240 - 420	16.0 - 24.0
<a href="#">Solvay Specialty Polymers Hyflon® F1750X Perfluoropolymer</a>	1.00e+17	270 - 440	17.0 - 26.0

Fig. 2. The first ten rows of the query results.

### GAMMA: validation method for gold

The following two validation steps were kept short and low level, that is, minimal and only to guide reproducibility, due to space limitation in this paper limitations. The entire user multi-manual regarding the existing market system [9,10] will contain all procedural specifications, pricing, consumable options, and software modules.

Industrial radiography was the best, most widespread, and most inexpensive laboratory-intensive method for non-destructive testing. Radiography fits very well with methodology clarification and commercialization.

The methodology was kept simple given its interdisciplinary nature, involving econophysics, coin casting, radiography, digital electronics, and statistics and programming in MATLAB-Python. Specific indicative MethodsX case study follows similar principles [2,6].

The steps to replicate this methodology are as follows:

1. Cast two sample golden coins [5].
2. Assemble a radiographic device.
3. Scan the two coins.
4. Perform a visual coin inspection.
5. Perform an analytical coin inspection.

**Table 6**

Properties of “Braskem UTEC® 6540 ultra high molecular weight polyethylene”

Physical properties	Metric
Specific Gravity	0.925 g/cc
Bulk Density	0.450 g/cc
Water Absorption	2.30%
Particle Size	225 Åµm
Viscosity Test	2800 cmÅ³/g
Molecular Weight	8.00e±6 g/mol
Mechanical properties	Metric
Hardness, Shore D	64
Tensile Strength at Break	≥= 30.0MPa
Tensile Strength, Yield	≥= 17.0MPa
Elongation at Break	>= 300 %
Izod Impact, Notched	NB
Charpy Impact, Notched	≥= 10.0 J/cmÅ²
Coefficient of Friction, Dynamic	0.09
Coefficient of Friction, Static	0.1
Abrasion	20
Electrical properties	Metric
Volume Resistivity	≥= 1.00e±14 ohm-cm
Surface Resistance	≥= 1.00e±12 ohm
Dielectric Constant	2.3
Dielectric Strength	90.0 kV/mm
Thermal properties	Metric
Heat of Fusion	68.34 J/g
CTE, linear	150 Åµm/m-Å°C
Specific Heat Capacity	2.01 J/g-Å°C
Thermal Conductivity	0.400 W/m-K
Deflection Temperature at 0.46 MPa (66 psi)	79.0 Å°C
Deflection Temperature at 1.8 MPa (264 psi)	48.0 Å°C
Vicat Softening Point	128 Å°C

*GAMMA.I-step: casting*

Fig. 3 depicts a demonstrative full-scale laboratory line with four sub-steps, each of which has two levels, as follows:

1. A torch heats the gold inside the lab tank to its melting point of 1064 degrees Celsius. Using an electronic temperature regulation gold melting resistance furnace in the lab or acquiring one from the professional market.
2. The melted gold is ejected into a small can or plate for cooling in an amorphous maze. There are various inexpensive silicon-type molds on the market.
3. A small portion of “antipodal fibers” will spread on the cooling surface. For dedicated applications, a “midi centrifuge for all types of separation processes” can be used.
4. The final gold bar or coin will reach the environmental temperature, ready for the test.

*GAMMA.II-step: Assembling a radiographic device*

The flat panel sensor from Hamamatsu is an efficient radiographic device in today’s market capable of scanning golden coins and banknotes [3]. This device was selected during pre-alpha realization tests and is the scanning device represented in the patent [10]. The scanned radiographic image, including image specifications, attributes and details, is shown in Fig. 4 exactly as produced in the specific commercial radiographic pad.

The current design demands 18 different voltages (20–90 VK) and multiple picture scanning. With a resolution of 2240 × 2.344, a full coin scan takes 18 s and requires 94 MB of storage. These 18 scanned pictures concern the same coin at different X-ray voltages. Photographs are comparable with each other. For example, photo no. 4 of one coin can only be compared with no. 4 of another.

The device to scan the golden coins shown in Fig. 5 has the following layout and six sub-steps:

1. The X-ray source emits low-level radiation toward the coin.
2. The golden coin has antipode elements.
3. A small digital scanner pad
4. A computer and frame grabber

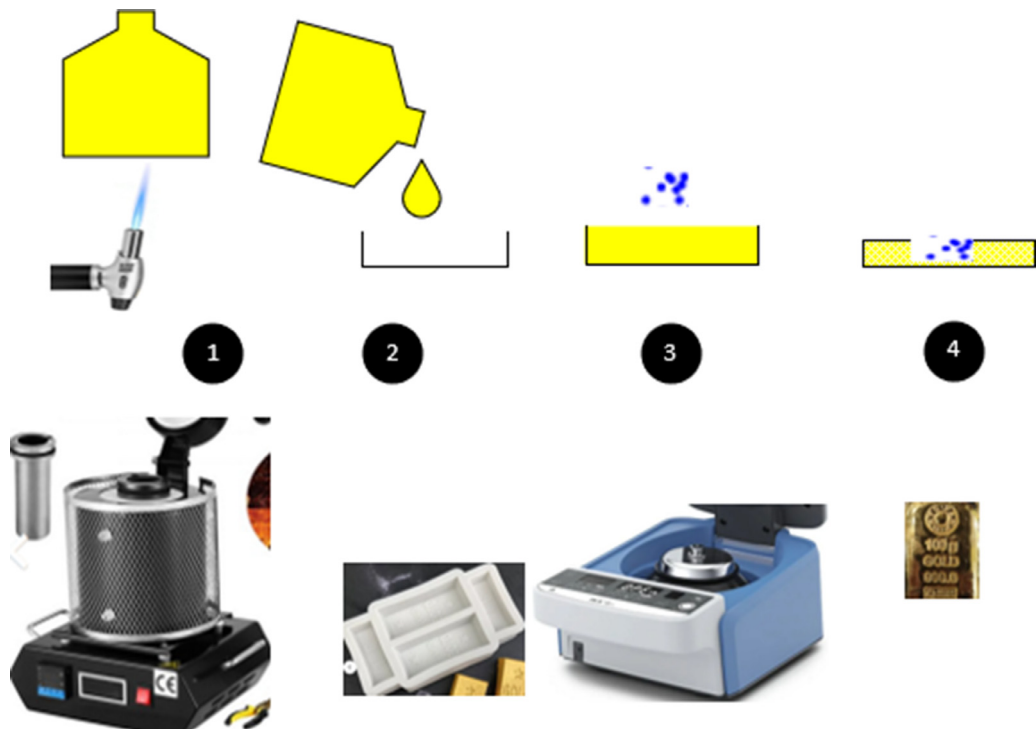


Fig. 3. Simple steps comprising an experiment for casting a primitive coin with antipode elements.

Parameter	Specifications	Unit
Pixel size	50 × 50	μm
Photodiode area	120 × 120	mm
Number of pixels	2400 × 2400	pixels
Number of active pixels	2240 × 2344	pixels
Readout	Charge amplifier array	-
Video output (Data1-12)	RS-422 (differential), 12-bit	-
Output data rate	15.15	MHz

Fig. 4. Scanned image specifications.

- 5. The image of the scanned coin in any image format
- 6. The scanned coin image files in digital format

The procedure follows arrows W1, W2, and W4.

GAMMA.III-step: scanning two coins

At GIII, the initial experiment entails scanning the same coin twice. The first and second scans are shown in Fig. 6, as plotted from the analytical results in MATLAB. All points represent the micro-elements of the selected micro-ingredient in the golden coin. Unfortunately, the casting procedure could be better regarding organizing the elements in a predefined order according to the traditional watermarked method. Fig. 9 shows the two images of the same coin.

Both scanned images were merged into a common picture to identify possible micro-differences, as shown in Fig. 7. A tiny discrepancy was found at (0.57, −0.78). These differences could be from a lower level of radiation concerning a significantly smaller micro-antipode element.

GAMMA-IV-step: analytical coin comparison in a MATLAB modeling experiment

The above image has 110 anomaly antipode ingredient points in the gold structure. For demonstration purposes, the first ten were selected from these 110 pairs of (x, y) elements, as shown in an array named A in Table 7. Based on a subsequent scan, array B was produced, showing antipode element differences at two radiographic points, up to three inequalities. All notation and calculations are made in MATLAB [8], but there are similarities in the PYTHON programming space. The next issue concerns the three inequalities



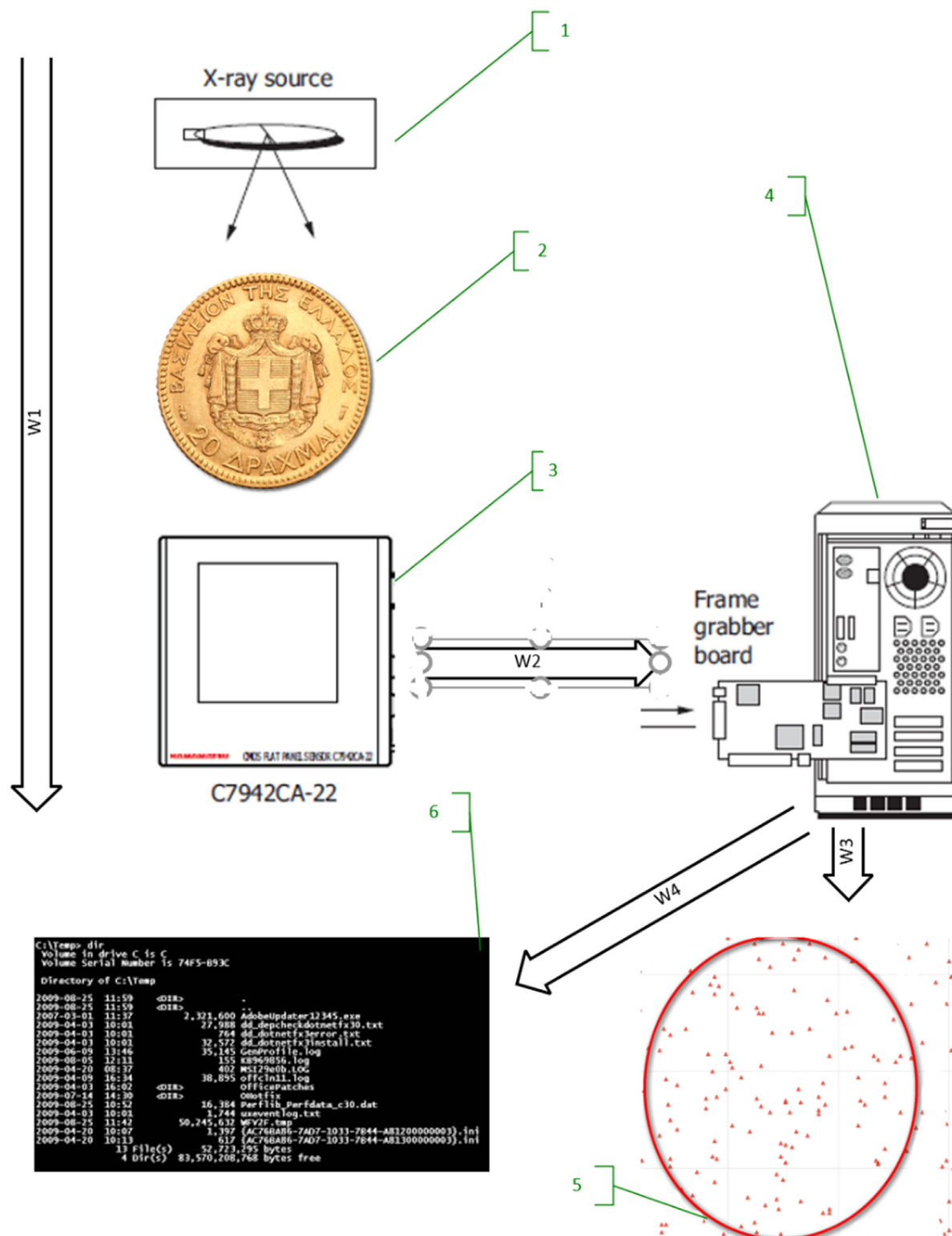


Fig. 5. Hardware for coin identification.



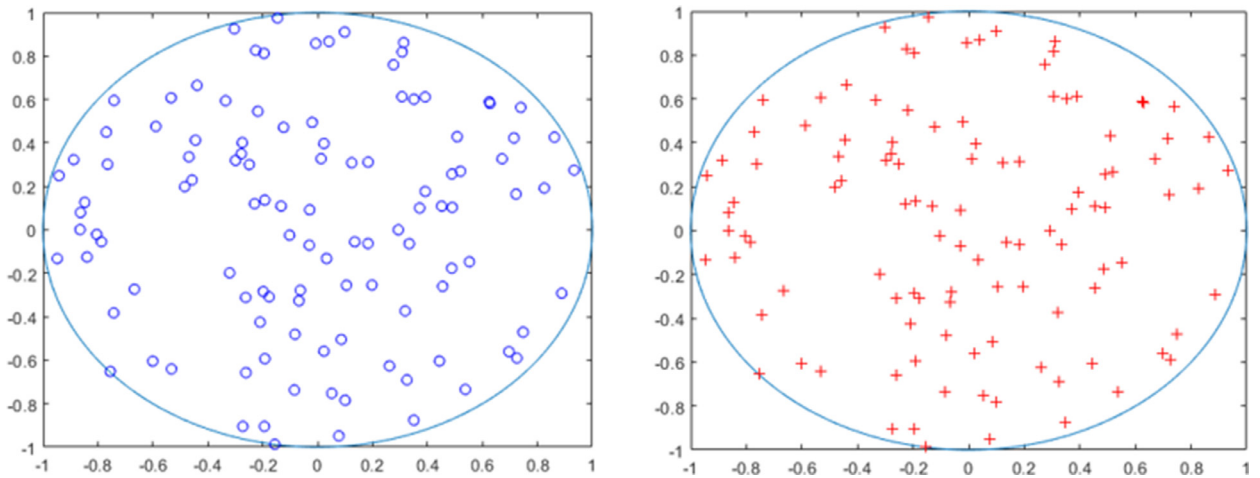


Fig. 6. Scanned images.

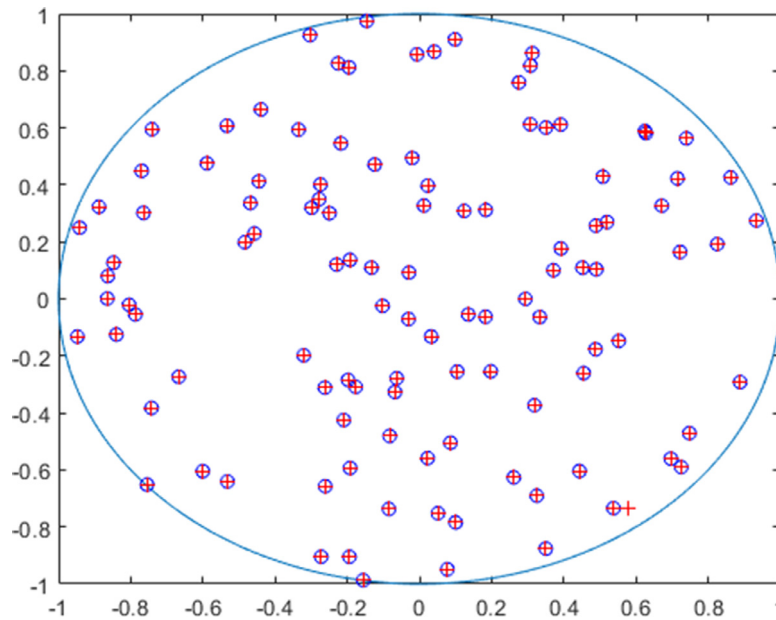


Fig. 7. Scanning the same golden coin.

**Table 7**

Arrays A and B with different scanned images.

---

A= [(0.53766714,-0.74169113), (0.86217332,0.426387557), (0.31876524,-0.372808742), (0.725404225,-0.590034564), (-0.063054873,-0.278064164), (0.714742904,0.422715691), (-0.124144348,0.471634326), (0.671497134,0.327059967), (0.48889377,0.257056157)]

B= [(0.53766714,-0.74169113), (0.86917332,0.427387557), (0.31876524,-0.372808742), (0.725404225,-0.590034564), (-0.063054873,-0.278064164), (0.714742904,0.422715691), (-0.124144348,0.471634326), (0.671497134,0.327059967), (0.48889377,0.27056157),]

---

and the exact layout of these discrepancies. The code below demonstrates the methodology for locating the differences always as a MATLAB screen in Table 7. Euclidean distance of two coins in MATLAB is  $d2st=(xs-yt)(xs-yt)'$  in Python  $math.dist(p, q)$ .

In Table 8 first the two different arrays are compared mathematically. Then the he standardized Euclidean distance calculation is calculated:  $d2st=(xs-yt)V^{-1}(xs-yt)'$ , where

- $V$  is the  $n$ -by- $n$  diagonal matrix with diagonal element given by  $(S(j))^2$
- $S$  is a vector of scaling factors for each dimension.

Each coordinate difference between observations is scaled by dividing by the corresponding element of the standard deviation.

**Table 8**

Normal and standardized Table 8. Euclidean Distance of Two CoPercentage Standardized Euclidean Di.

A<B
ans = 9 × 2 logical array
0 0
1 1
0 0
0 0
0 0
0 0
0 0
0 0
0 0
0 1
<b>Exact coordinates difference</b>
A-B
ans = 9 × 2
0 0
-0.0070 -0.0010
0 0
0 0
0 0
0 0
0 0
0 0
0 -0.0135
[Coin_euclidian,I] =pdist2(A,B,'euclidean','Smallest',1);
Coin_euclidian = 1 × 9
0 0.0071 0 0 0 0 0 0 0.0135
[Coin_Standardized_Euclidean,I] =pdist2(A,B,'seuclidean','Smallest',1);
Coin_Standardized_Euclidean = 1 × 9
0 0.0201 0 0 0 0 0 0 0.0279

**Table 9**

Hamming distance (Percentage of differing coordinates), Chebychev distance (maximum coordinate difference).

[Coin_hamming_Distance,I] =pdist2(A,B,'hamming','Smallest',1);
Coin_hamming_Distance = 1 × 9
0 1.0000 0 0 0 0 0 0 0.5000
[Chebychev_distance,I] =pdist2(A,B,'chebychev','Smallest',1);
Chebychev_distance = 1 × 9
0 0.0070 0 0 0 0 0 0 0.0135

There are a lot of different calculations to be evaluated. Hamming distance is shown in Table 9  $dst=(\#(x_{sj} \neq y_{tj}))/n$ , along Chebychev distance, a special case of the Minkowski distance, where  $p$  reaches infinitive  $dst=\max_j\{\downarrow x_{sj}-y_{tj}\downarrow\}$ .

The exact methodology used to locate the discrepancies and the golden coin serial number and identity are at the discretion of the machine operator.

## DELTA: antipodal method validation for paper

### DELTA-I-step: handmade paper sheet infused with antipodal ingredients

The initial step to prepare the paper sheet is shown in Fig. 8, with six sub-steps.

1. A normal paper sheet is cut and put with water in an *in vitro* diagnostic device. A small torch underneath may facilitate pulp formulation.
2. The selected antipodal ingredients are placed inside the *in vitro* can.
3. A small lab mixer stirs the pulp for a while.
4. The pulp is passed through a flat strainer.
5. The pulp is left to dry for days (alternatively, a professional hot air dryer laboratory oven may be used) until the formation of the final product.
6. The final result is a piece of paper with scattered antipodal ingredients.



Fig. 8. Primitive laboratory creation of a piece of paper infused with antipodal ingredients.

#### DELTA-II-step: Lab X-RAY machine

The antipode-enriched paper (Figs. 9, 6) is scanned on the integrated commercial-ready device (7,8,9). Two different scans produce two different digital paper–sulfur distinction antipode points, as plotted in Fig. 11 sub-diagrams 20 and 21. Digital analytics revealed three discrepancies. The combined diagram 22 shows these discrepancies at the two red arrows and the blue arrow.

#### DELTA-III-step: raw data direct sensor comparison using artificial intelligence tools

This final step is devoted to digital electronics and programming aficionados. It is proposed as an industrial-academic experiment and is still in the pre-alpha implementation phase of antipodal non-destructive testing (NDT) applications. Fig. 10 clarifies the methodology with a consecutive phase and/or devices:

6. The antipodal ingredient-infused paper banknote.
7. An appropriate X-ray source.
8. The photodiode array pad producing analog data (device photo).
9. Schematics for an X-ray static detector [9999]
10. The computer
11. Multidimensional data science structure to store all previous, current, and future paper layouts.

In the preliminary alpha testing phase, synthetic data were necessary to verify the method. To predefine those data, more profound knowledge of the scanning area was necessary. All radiographic scanners use a small or large photodiode area and generate an image. Regarding scanning the gold coin as described above, the scanned image is sent from the large photodiode pad to the image construction board, and the computer system processes it using image recognition methods.

Several commercially-available photodiode X-ray panels offer the flexibility and traceability necessary for scanning high-value items. The exact configuration of a typical large photodiode pad is as follows:

- The system comprises a sensor board (8) and the control board(9).
- The sensor board contains a CMOS image sensor chip comprising a two-dimensional photodiode array, a row-scanning vertical shift register, and several charge amplifier's arrays.
- Each charge amplifier array has a horizontal shift register and consists of multi-channel charge amplifiers, possibly with CDS circuits.

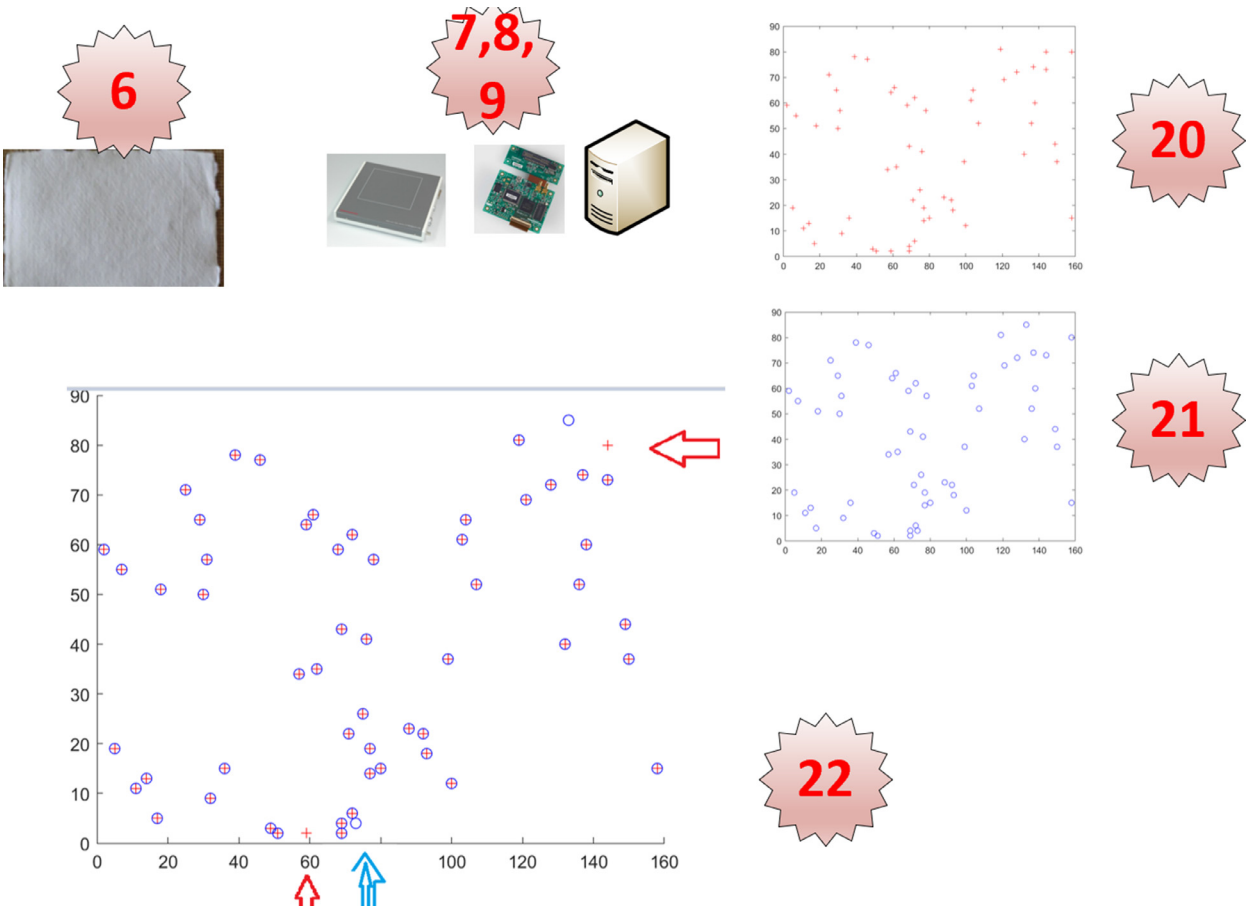


Fig. 9. The device is tailored for raw data capture of banknotes.

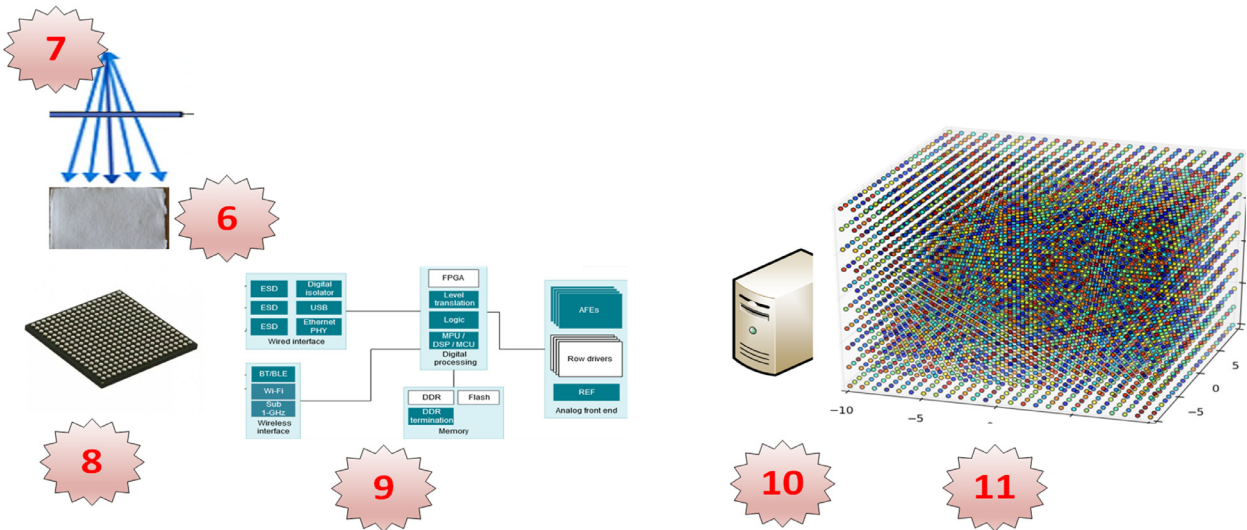


Fig. 10. Raw digital big data from the radiographic pad.

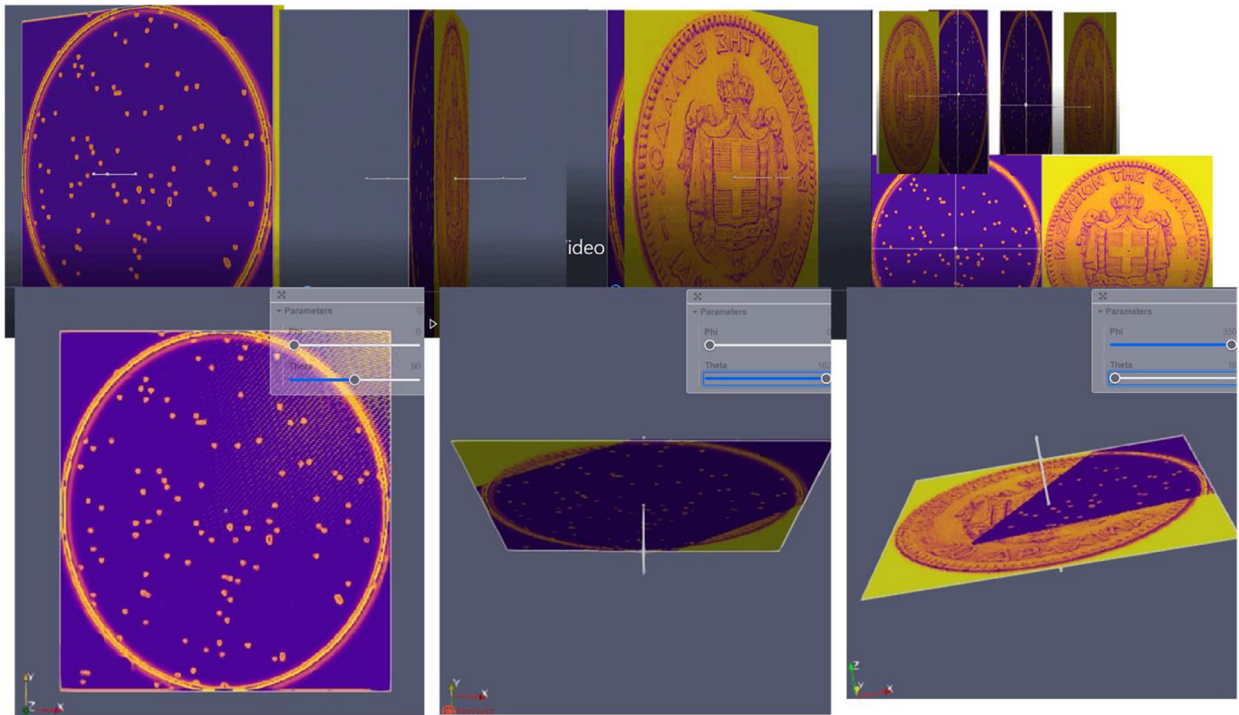


Fig. 11. Interactive Visualization tool and associated tilt videos for Gold coin.

At the final stage, shown in Fig. 12, the control board converts the analog signal into a digital signal. Using the above proposed MethodsX approach to capture raw sensor data, this analog signal does not drive the frame grabber. Instead, it feeds the computer producing the big data structured schema. Every scanned paper sheet is uniquely digitally represented by a simple multidimensional array. This array is easily manipulatable using the current pure data analytics, not image recognition, methodologies.

Such computer board customization exceeds the scope of fellow researchers' and technicians' method replication, but new developments arise after thoroughly analyzing the new real-world trends. Implementation discussion could include the following:

- Dominant players with a monopoly do not allow digital electronics easy riders to play with their highly reputed systems.
- The sensor and photodiode market are limited. The real profit comes from research services. IBM once had a monopoly, and it is still profitable.
- All computer and technology giants started in a small garage.

### Interactive visualization tools

The laboratory-detailed implementation steps are the heart of this research. Generally, we do not endorse that “Media is the Message” but we have to respect equally both research and educational faces of our works. In order for the average reader to read this research two types of tools are provided in a secondary dataset [12]. The TOMVIZ software [13] main feature is the coupled side of the dataset. There is nothing more coupled than the embedded antipode distinguishability fibres inside coins and bank-notes. From this full interactive visual supplement dataset [12] we selected a few static frames depicted in Fig. 11 for gold and Fig. 12 for banknotes. Static frames concern both demonstration videos and interactive visualization through three dimensional axes, phi/theta angle pairs (Greek  $\varphi, \theta$ ).

At this moment video and visualization files need to be downloaded and run locally [11]. Mendeley Dataset will cover direct online access in the near future.

### Research extension and usability

The above research concerns gold and banknotes, but it is helpful for any counter-forgery methods. Very quickly, any tangible artificial market item could be uniquely identified. For example, an electric kitchen could have inside a giant magnetic fingerprint. A simple scanner informs the seller, the accountant, the owner, and the service man which specific kitchen exactly is, among the million. Some researchers would think of similar methodologies for medicine and food, but we strongly disagree as unethical. We hope that legislation will continue to protect us for eternity.



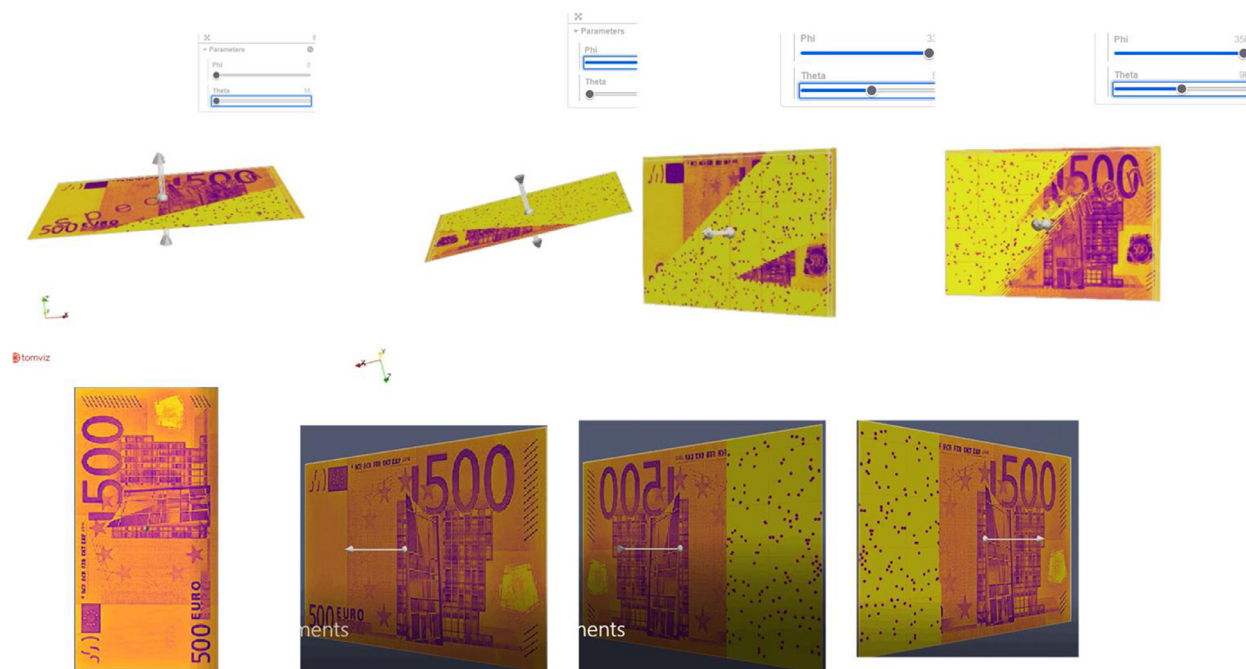


Fig. 12. Interactive Visualization tools and an associate tilt video for Paper bank-note.

## Ethics statements

null

## Declaration of interests

Please tick the appropriate statement below (please do not delete either statement) and declare any financial interests/personal relationships which may affect your work in the box below.

The authors declare that they have no known competing financial interests or personal relationships that could have appeared to influence the work reported in this paper.

The authors declare the following financial interests/personal relationships which may be considered as potential competing interests: Please declare any financial interests/personal relationships which may be considered as potential competing interests here.

## CRediT authorship contribution statement

**Athanasios Zisopoulos:** Conceptualization, Methodology, Software, Formal analysis, Writing – original draft, Writing – review & editing, Visualization, Funding acquisition. **Georgia Broni:** Conceptualization, Investigation, Supervision. **Nikos Kartalis:** Resources, Project administration. **Konstandinos Panitsidis:** Software.

## Data Availability

[1] [dataset] Zisopoulos, Athanasios (2021), “ANTIPODAL MATERIAL dataset”, Mendeley Data, V2, doi: 10.17632/mgr25gs4k6.2, <https://data.mendeley.com/datasets/mgr25gs4k6>

## Acknowledgments

This research did not receive any specific grant from funding agencies in the public, commercial, or not-for-profit sectors.

Zisopoulos Athanasios granted recently two patents from WIPO:

Gold bullion origination and verification system with unique identification by embedding traceable ingredients Grant Number 1010167, Grant Date 31.01.2022 [https://patentscope.wipo.int/search/en/detail.jsf?docId=GR356981880&\\_cid=P11-L8G199-08661-1](https://patentscope.wipo.int/search/en/detail.jsf?docId=GR356981880&_cid=P11-L8G199-08661-1)

Paper pulp methodology for production of unique paper sheets and banknotes embodied with exclusivity antipode trace elements, Grant Number 1010230 Grant Date 06.05.2022 [https://patentscope.wipo.int/search/en/detail.jsf?docId=GR367948438&\\_cid=P11-L8G199-08661-1](https://patentscope.wipo.int/search/en/detail.jsf?docId=GR367948438&_cid=P11-L8G199-08661-1)

## Supplementary materials

Supplementary material associated with this article can be found, in the online version, at doi:10.1016/j.mex.2022.101981.

## References

- [1] Zisopoulos, Athanasios (2021), "Antipodal material dataset", Mendeley Data, V2, DOI: 10.17632/mgr25gs4k6.2, <https://data.mendeley.com/datasets/mgr25gs4k6/1>
- [2] A. du Plessis, P. Sperling, A. Beerlink, W.B. du Preez, S.G. le Roux, Standard method for microCT-based additive manufacturing quality control 4: metal powder analysis, *MethodsX* 5 (2018) 1336–1345, doi:10.1016/j.mex.2018.10.021.
- [3] Hamamatsu, 2022. Related documents | for non-destructive inspection | Hamamatsu photonics. URL: [https://www.hamamatsu.com/eu/en/product/optical-sensors/x-ray-sensor/x-ray-flat-panel-sensor/x-ray-flat-panel-sensors-for-nondestructive-inspection/related\\_documents.html](https://www.hamamatsu.com/eu/en/product/optical-sensors/x-ray-sensor/x-ray-flat-panel-sensor/x-ray-flat-panel-sensors-for-nondestructive-inspection/related_documents.html).
- [4] Matweb, (2022) *Search engineering material by property value*. (n.d.). Retrieved September 27, 2022, from <https://www.matweb.com/search/PropertySearch.aspx>
- [5] E. Tsiatsiou, Electrum-g, a tangible coin actualization schema: patents for casting, forensics and trade options, *Bus. Econ. Res.* 10 (2020) 182–195 URL: <https://www.macrothink.org/journal/index.php/ber/article/view/16094>, doi:10.5296/ber.v10i1.16094.
- [6] C.A.T. Toloza, J.M.S. Almeida, S. Khan, Y.G. dos Santos, A.R. da Silva, R.Q. Aucélio, Kanamycin detection at graphene quantum dot-decorated gold nanoparticles in organized medium after solid-phase extraction using an aminoglycoside imprinted polymer, *MethodsX* 5 (2018) 1605–1612, doi:10.1016/j.mex.2018.11.019.
- [7] Unknown (Texas Instruments) (2022). (n.d.). X-ray systems design resources | TI.com. Retrieved October 11, 2022, from <https://www.ti.com/solution/x-ray-systems?variantid=28540#block-diagram>
- [8] Unknown (Matlab) (2002), Pairwise distance between pairs of observations - MATLAB pdist. (n.d.). Retrieved October 11, 2022, from [https://www.mathworks.com/help/stats/pdist.html?s\\_tid=mwa\\_osa\\_a](https://www.mathworks.com/help/stats/pdist.html?s_tid=mwa_osa_a)
- [9] Zisopoulos A., (2022) *GR1010230 paper pulp methodology for production of unique paper sheets and banknotes embodied with exclusivity antipode trace elements*. (n.d.). Retrieved September 24, 2022, from [https://patentscope.wipo.int/search/en/detail.jsf?docId=GR367948438&\\_cid=P11-L8G199-08661-1](https://patentscope.wipo.int/search/en/detail.jsf?docId=GR367948438&_cid=P11-L8G199-08661-1) Grant Number 1010230 Grant Date 06.05.2022
- [10] Zisopoulos A., (2022), *GR1010167 gold bullion origination and verification system with unique identification by embedding traceable ingredients*. (n.d.). Retrieved September 24, 2022, from [https://patentscope.wipo.int/search/en/detail.jsf?docId=GR356981880&\\_cid=P11-L8G199-08661-1](https://patentscope.wipo.int/search/en/detail.jsf?docId=GR356981880&_cid=P11-L8G199-08661-1) Grant Number 1010167, Grant Date 31.01.2022
- [11] A. Zisopoulos, MIDAS, repository with under the pillow gold using antipodal unique identification of golden coins for regional development and monetary applications, *Rev. Int. Geogr. Educ.* 12 (01) (2021) 2022 [https://papers.ssrn.com/sol3/papers.cfm?abstract\\_id=4092050](https://papers.ssrn.com/sol3/papers.cfm?abstract_id=4092050).
- [12] Zisopoulos, A. (2022), "Interactive visualization tools for antipode ingredients inside gold and banknotes", Mendeley Data, V1, doi: 10.17632/6d25rpvwtb.1 <https://data.mendeley.com/datasets/6d25rpvwtb/1>
- [13] J. Schwartz, C. Harris, J. Pietryga, et al., Real-time 3D analysis during electron tomography using tomviz, *Nat. Commun.* 13 (2022) 4458, doi:10.1038/s41467-022-32046-0.